4105-PPI LEDoS Pixel Circuit With an Analog Pulse-Width-Modulation Driving Method Employing a Dual-Sweep Signal for Wider Data Range

Chanjin Park, Kyeong-Soo Kang*, Yumin Yun*, Sae-Ru Cheon*, and Soo-Yeon Lee**
***Department of Electrical and Computer Engineering, Seoul National University, Seoul, South Korea**

Abstract
In this paper, a 4015-pixel per inch light emitting diode on silicon pixel circuit and its driving method for a wider data range are proposed. The proposed method adopts a SWEEP[n] signal that ramps up two different voltage ranges to address the narrow data range of complementary metal-oxide-silicon pixel circuits. By employing the method, the data range is extended by 107.7% compared to the conventional method using a single-sweep SWEEP[n] signal. As the proposed method does not require a complex pixel structure, it can be implemented with a simple structure.

Author Keywords
Augmented reality; Complementary Metal-Oxide-Silicon Field Effect Transistor; Pulse-Width-Modulation; MicroLED; Data Range;

1. Introduction
As augmented reality (AR) and virtual reality (VR) devices are gaining a widespread attraction, the demand for microdisplays with higher resolutions is rapidly increasing. To produce realistic images in AR/VR devices, microdisplays with several thousand pixels per inch (PPI) are required. However, conventional display backplanes based on thin-film transistors (TFTs) are unable to reach this level of pixel density due to the size limitation of TFTs. To overcome this, microdisplays now employ metal-oxide-silicon field-effect transistors (MOSFETs) with sub-micrometer channel lengths [1],[2],[3].

While VR devices are predominantly used indoors, AR devices are designed for outdoor environments, as well. This requires AR microdisplays to exhibit not only high luminance and ambient contrast ratios but also maintain consistent performance across varying temperatures. Compared to organic-light emitting diodes (OLEDs), micro-light emitting diodes (μLEDs) offer higher maximum luminance and external quantum efficiency, and are free from burn-in issues [4],[5], making them particularly suitable for AR applications. However, μLEDs can have wavelength shift according to their current density [6],[7], which can lead to color degradation. Thus, μLED backplanes require pulse-width-modulation (PWM) driving method to prevent color instability.

However, integrating μLED with complementary-MOSFET (CMOS) backplanes needs to address the challenges of narrow operating voltage. Due to the small operation voltage of CMOS, CMOS pixel circuits typically utilize a very narrow data range of less than 1 V [3],[8],[9]. This introduces a significant burden in data driver circuits, as they need to split the data voltage range into very small voltage intervals to accurately represent a target gray level. Therefore, expanding the data range is critical to accurately express gray levels in CMOS-based microdisplays.

To address this issue, several methods for OLED-on-silicon (OLEDoS) microdisplays have been proposed. One approach involves voltage division using multiple capacitors [3],[8],[10]. However, employing several capacitors increases the size of the pixel circuit, which can decrease the image quality in AR devices.

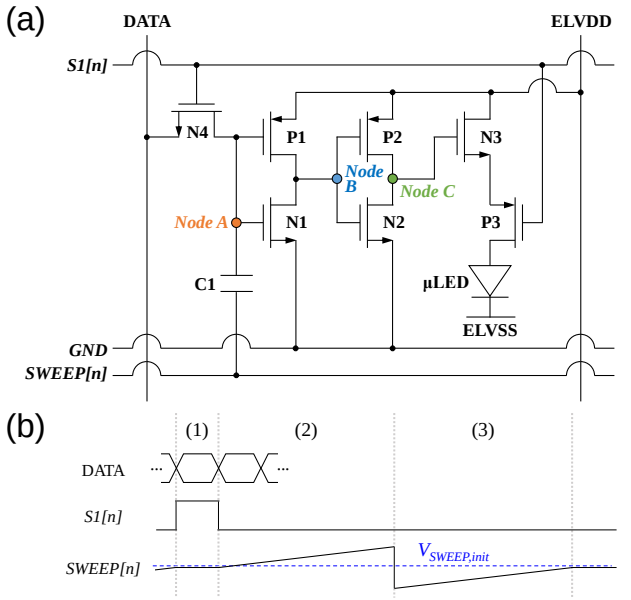

Figure 1. (a) The proposed CMOS-based μLED pixel circuit and (b) its timing diagram

Another approach is to place an active load in the OLED current path [9],[11]. The added active load gives the effect of increased subthreshold swing (S.S), enabling smaller current variation between the data. However, this approach is not suitable for μLED displays, as they use the PWM driving method. The increased S.S in the PWM unit can lead to longer rising or falling times, potentially causing color distortion, especially in low gray levels [12]. As a result, CMOS-based μLED microdisplay requires a novel approach, different from the methods previously proposed for OLEDoS microdisplay, to achieve a wider data range.

In this paper, 4015 PPI light emitting diode on silicon (LEDoS) pixel circuit with a new driving method that employs a dual-sweep SWEEP[n] signal that toggles twice with different voltage values for wider data range are proposed. The operation of the pixel circuit and its driving method is verified through the simulation conducted through HSPICE with CMOS model based on 1.8 V 0.18 μm CMOS fabrication process. By employing the proposed method, the data range is expanded by 107.7% compared to the pixel circuit employing the conventional SWEEP[n] signal, which only toggles once during the emission stage. As the proposed method does not need a complicated structure, the proposed LEDoS pixel circuit could achieve 4051 PPI with an area of 2.1 μm × 6.3 μm.

2. Pixel Circuit and Its Operation
Fig. 1(a) illustrates the schematic of the proposed CMOS-based μLED pixel circuit, which consists of 7 transistors and 1 capacitor. In the circuit, P1 and N1 form inverter 1, whereas P2 and N2 form inverter 2. The operation of the circuit is divided into

ISSN 0097-996X/25/5601-0572-$1.00 © 2025

Table 1. Parameters used for the simulation

Device parameters		Signal parameters	
N1 *(W/L)*	0.5 µm/ 0.18 µm	ELVDD / ELVSS	1.8 V / -2 V
		$V_{SWEEP,init}$	0.85 V
N2 to 4, P1 to 4 *(W/L)*	0.22 µm/ 0.18 µm	V_{SWEEP}	1.7 V to 0 V
		S1[n]	1.8 V to 0 V
C1	10 fF	$V_{body,p}$ / $V_{body,n}$	1.8 V / 0 V

*W: width of transistor, L: length of transistor
** $V_{body,p}$: body voltage of PMOS, $V_{body,n}$: body voltage of NMOS

three stages: (a) data input, (b) emission 1, and (c) emission 2, as shown in fig. 1(b).

(1) Data input stage: In this stage, data voltage (V_{DATA}) is applied to node A, while the lower node of C1 is biased with $V_{SWEEP,init}$. As a result, the voltage stored in C1 (V(C1)) becomes $V_{DATA} - V_{SWEEP,init}$. During this stage, P3 remains off, preventing the µLED from emitting light.

(2) Emission 1 stage: As V_{SWEEP} increases linearly, the voltage of node A (V_A) also increases until it reaches the maximum V_{SWEEP}. Initially, when V_A is low, voltage of node B (V_B) is high, keeping the voltage of node C (V_C) low. As a result, N3 remains off, and the µLED does not emit light. However, once V_A reaches the transition point of inverter 1 (V_{M1}), inverter 1 is in the pull-down condition, and V_C is pulled up to ELVDD, turning M3 and beginning light emission.

However, for high V_{DATA} values, V_A already exceeds V_{M1} from the beginning, keeping the µLED on throughout the emission 1 stage. Therefore, this stage controls the gray levels using low V_{DATA}, allowing for expressing low gray levels.

(3) Emission 2 stage: At the beginning of this stage, V_{SWEEP} switches to the minimum V_{SWEEP}, then increases linearly back to $V_{SWEEP,init}$. This operation initially turns M3 off, stopping the emission. However, as V_{SWEEP} increases again, µLED is turned on at different times depending on V(C1). Since the V_{SWEEP} of the emission 2 stage is much lower than in the emission 1 stage, V_A does not exceed V_{M1} at the beginning of this stage, allowing for different pulse widths based on higher V_{DATA} levels. Thus, emission 2 stage determines the gray levels using high V_{DATA}, allowing for expressing high gray levels.

The reason for utilizing the dual-sweep SWEEP[n] signal, one for low V_{DATA} and the other for high V_{DATA}, is to avoid the side effects of low and high V_{DATA} ranges under the single sweep SWEEP[n] signal. The effectiveness of the dual-sweep SWEEP[n] signal for wider data range is verified by comparing the proposed method and conventional methods 1 and 2.

3. Result and Discussion

To verify the performance of the proposed pixel circuit and its driving method, simulations are conducted through HSPICE using CMOS devices based on 1.8 V 0.18 µm CMOS process. The specific parameters used in the simulations are summarized in Table 1.

Fig. 2(a) and (b) present the simulated transient µLED current ($I_{µLED}$) waveforms of the proposed pixel circuit under the low V_{DATA} range and high V_{DATA} range, respectively. During the emission 1 stage, µLED continuously emits light throughout the entire stage for high V_{DATA}, while the µLED pulse width varies for low VDATA, as mentioned in Section 2. Conversely, during the emission 2 stage, the µLED does not emit light for low V_{DATA},

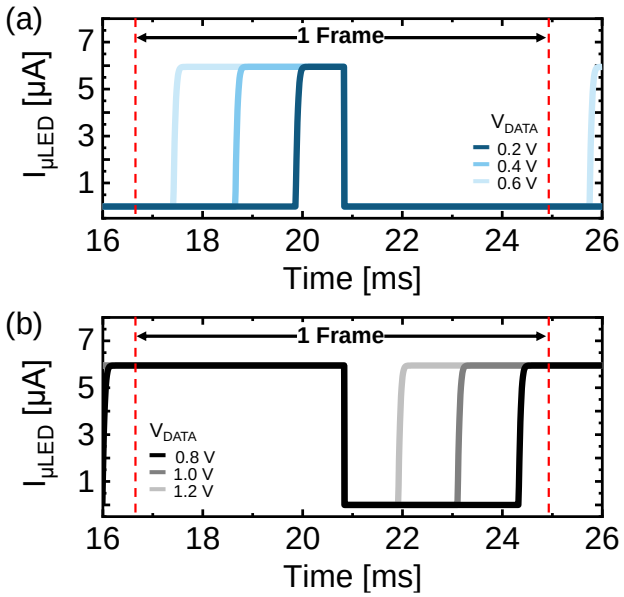

Figure 2. Transient waveform of µLED of the proposed pixel circuit (a) with low V_{DATA} and (b) with high V_{DATA}.

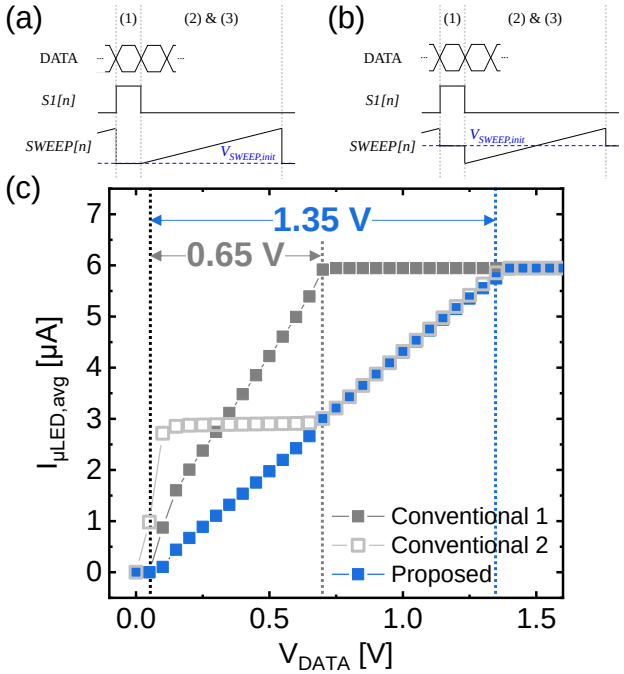

Figure 3. Timing diagram of the conventional operation (a) 1 and (b) 2, and (c) the average µLED current of the proposed pixel with the proposed operation and the conventional operations according to V_{DATA}.

while the µLED pulse width changes for high V_{DATA}. This demonstrates that the proposed pixel circuit can implement the proposed PWM driving operation, generating $I_{µLED}$ pulse with different widths based on V_{DATA}.

To evaluate the data range expansion of the proposed PWM driving method, it was compared with the conventional driving methods, having only one emission stage with a continuously increasing SWEEP[n] signal during the emission stage. For the consistent comparison, other signals remain unchanged in conventional methods 1 and 2. The timing diagrams of signals

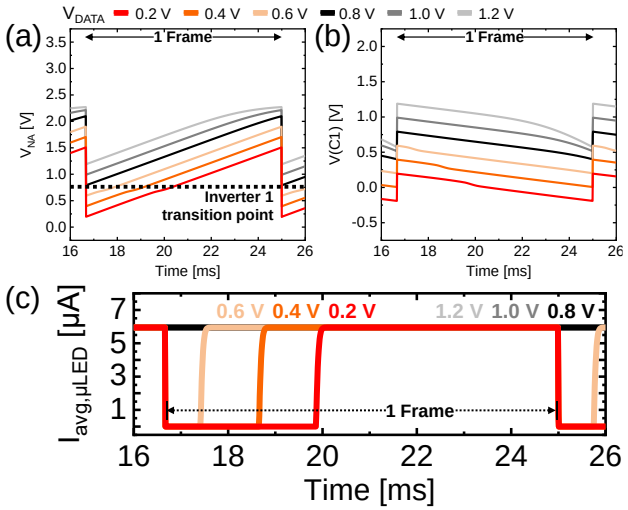

Figure 4. Transient waveform of (a) V_A, (b) V(C1) and (c) $I_{\mu LED}$ of the proposed pixel circuit under conventional method 1 according to V_{DATA}.

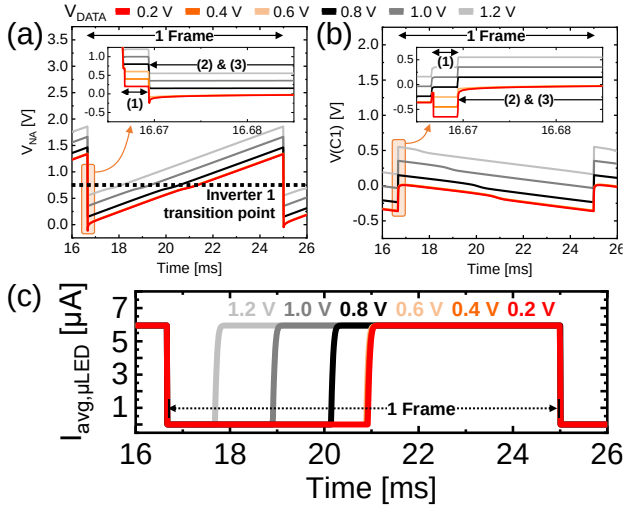

Figure 5. Transient waveform of (a) V_A and (b) V(C1) and (c) $I_{\mu LED}$ of the proposed pixel circuit under conventional method 2 according to V_{DATA}.

used for conventional method 1 and 2 are shown in fig. 3(a) and (b), respectively. Fig. 3(c) illustrates the average $I_{\mu LED}$ ($I_{avg,\mu LED}$) of one frame. While the proposed method and two conventional methods all show an increase in $I_{avg,\mu LED}$ with higher V_{DATA}, the proposed method achieves a significantly wider data range compared to the conventional methods. In conventional method 1, the data range is limited to low voltage levels from 0.05 V to 0.7 V. In conventional method 2 while high gray level is adjusted with $V_{DATA} > 0.7$ V, low gray levels cannot be expressed. Detailed explanation on these mechanisms are explained in following sections. As a result, only high V_{DATA} can be utilized with conventional method 2. In contrast, the proposed method can utilize both high and low V_{DATA} levels through the proposed dual-sweep SWEEP[n] signal, extending the data range to approximately 1.35 V. Compared to the conventional method 1, the data range is extended by 107.7%. Detailed explanations on mechanism of data ranges for each method are explained in following sections.

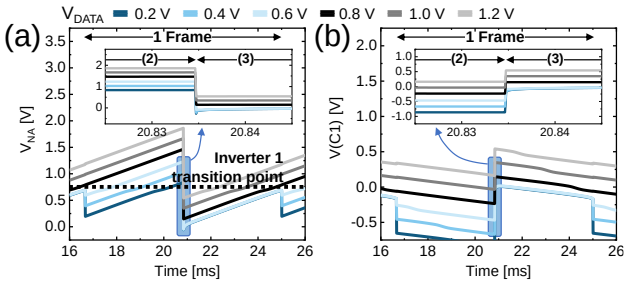

Figure 6. Transient waveform of (a) V_A and (b) V(C1) of the proposed method according to V_{DATA}.

3.1. Narrow data range of conventional method

The narrow data range of conventional method 1 arises from V_A exceeding V_{M1} before the emission stage begins, for high V_{DATA}, as shown in fig 4(a). During the emission stage, V(C1) for each V_{DATA} differs, indicating V_{DATA} is well stored in C1 during the data input stage, as shown in fig. 4(b). However, the pulse width of $I_{\mu LED}$ is identical for V_{DATA} = 0.8 V, 1.0 V and 1.2 V, as shown in fig. 4(c). This is due to the μLED already emitting light at the start of the emission period when V_{DATA} over 0.6 V is utilized. Consequently, the control of pulse width for high V_{DATA} becomes challenging.

High V_{DATA} can be utilized by increasing $V_{SWEEP,init}$, as in conventional method 2. With higher $V_{SWEEP,init}$, overall V_A level decreases during the emission stage compared to when a lower $V_{SWEEP,init}$ is used, as shown in fig. 5(a). This is because smaller voltage is stored in C1 during the data input stage, as shown in fig.5(b). This prevents the μLED from emitting light at the beginning of the emission stage even with high V_{DATA}, having different emission starting time based on V_{DATA}. However, the pulse width of $I_{\mu LED}$ for V_{DATA} = 0.2, 0.4 V and 0.6 V are nearly identical, as shown in fig 5(c). This indicates that the PWM operation is not implemented with these V_{DATA} values, potentially causing clipping in low gray levels. When a higher $V_{SWEEP,init}$ is employed, V(C1) for low V_{DATA} is lost when V_{SWEEP} decreases from $V_{SWEEP,init}$ to 0 V at the beginning of the emission stage, as shown in fig. 5(b). If V_{DATA} is smaller than $V_{SWEEP,init}$, the V(C1) becomes negative. In this case, V_A should ideally drop below 0 V as V_{SWEEP} decreases to 0 V, specifically to $V_{DATA} - V_{SWEEP,init}$. However, V_A only decreases until V_A reaches 0 V, as shown in fig. 5(a). This arises from the off-voltage of N4. When the gate-source voltage of N4 exceeds its off-voltage, N4 turns on and operates in the saturation region. As a result, V_A cannot drop below the gate voltage of N4, which is 0 V, causing the stored V_{DATA} in C1 to be lost. This inhibits the intended low current level from being achieved.

3.2. Proposed method for wider data range

As discussed earlier, the data range of conventional methods 1 and 2 are limited to the high V_{DATA} level and low V_{DATA}, respectively. While factors that limit the expansion of the data range of conventional methods also occur during the proposed method, the proposed method successively extended the data range without clipping in grayscale expression by separating the emission stages for high V_{DATA} and low V_{DATA}. Fig. 6 shows the transient waveform of V_A and V(C1) of the proposed pixel circuit employing the proposed method. During the emission 1 stage, the pixel circuit operates similarly to the convention method 1. With high V_{DATA}, V_A already exceeds V_{M1}, enabling μLED emission from the beginning, as shown in fig. 6(a). As a result, the $I_{\mu LED}$ pulse width is controlled only with low V_{DATA}. During this period,

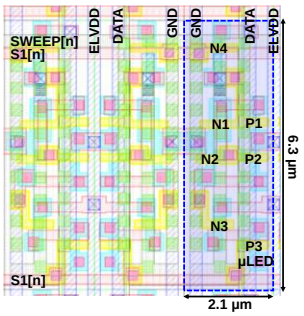

Figure 7. The layout of the proposed pixel circuit using 1.8 V 0.18 μm CMOS fabrication process. Single subpixel is marked with blue.

V(C1) is preserved for all V_{DATA}. When entering the emission 2 stage, V_{SWEEP} decreases rapidly to a voltage level smaller than $V_{SWEEP,init}$. This leads to the clipping in V(C1) for low V_{DATA}, similar to the conventional 2 method, as shown in fig. 6(b). However, low gray level expression is not affected by this clipping. Unlike the conventional 2 method, the current pulse utilizing low V_{DATA} is already generated during the emission 1 period. Also, μLED does not emit light for low gray levels, during the emission 2 stage. Therefore, the pixel circuit can generate the intended $I_{\mu LED}$ pulse as long as long as the V_A of low V_{DATA} is below V_{M1} during the emission stage 2 to stop μLED from emitting light. These results demonstrate that the data range can differ by the waveform of the SWEEP[n] signal, even when the sweep range is the same.

Fig. 7. shows the layout of the proposed pixel circuit. As the proposed method eliminates the need for additional transistors or capacitors, the resolution of 4051 PPI was achieved, with an area of 2.1 μm × 6.3 μm. With the flipped structure, nearby pixel circuits shared P-implant or N-implant, increasing the area efficiency.

4. Conclusion

This paper proposes a 4015-pixel PPI LEDoS pixel circuit and its driving method for a wider data range. The proposed driving method employed a dual-sweep SWEEP[n] signal with 2 emission stages, each emission stage generating $I_{\mu LED}$ pulse for low V_{DATA} and high V_{DATA}. To verify the pixel circuit and its driving method, simulations were conducted using HSPICE with a CMOS model based on a 1.8 V 0.18 μm CMOS process. The proposed pixel circuit employing the proposed driving method showed variation in pulse width with different V_{DATA}, showing that the proposed circuit is capable of PWM operation. Furthermore, the data range of the pixel circuit is expanded by 107.7% under the proposed driving method without clipping in grayscale expression, compared to the conventional method. This improvement was due to utilizing both high and low V_{DATA} levels, whereas conventional methods could utilize only one V_{DATA} level. As the pixel circuit can have a wider data range without complicated structure, the proposed pixel circuit achieved a pixel area of 2.1 μm × 6.3 μm.

5. Impact of the research

Proposed LEDoS pixel circuit and its driving method effectively controlled the pulse width of $I_{\mu LED}$, verifying their ability to implement PWM driving. Also, by employing the dual-sweep SWEEP[n] signal, the data range of the pixel circuit effectively increase without the need for additional transistors and capacitors, achieving high resolution.

6. Acknowledgements

The EDA tool was supported by the IC Design Education Center(IDEC), Korea.

7. References

1. Tingzhou M, Yuan J, Yin Z, Xingyan L, Xinjie H, Feng R, Field Stack Lighting Driving Method for Low Power Organic Light Emitting Diode-on-Silicon Microdisplay. *IEEE Journal of Selected Topics in Quantum Electronics*; 2024, 30(2): 2000511
2. Jang J, et al. High-luminance, large-size 4K OLED microdisplays for VR/MR applications. *Journal of the Society for Information Display*; 2024, 32(5): 371 – 378
3. Shin-Song C, Paul C.-P. C. An Ultra-High 6318-PPI Pixel Circuit for Micro-OLED Displays With V_{th} Compensated up to 10-bit Gray Levels. *IEEE Journal of Solid-State Circuits*; 2024, 59(7): 2236 – 2247
4. Yuge H, En-Lin H, Ming-Yang D, Shin-Tson W. Mini-LED, Micro-LED and OLED displays: present status and future perspectives. *Light: Science & Applications*; 2022, 9(1): 105.
5. Tingzhu W, et al. Mini-LED and micro-LED: promising candidates for the next generation display technology. *Applied sciences*; 2018, 8(9): 1557.
6. Shijie Z, et al. Characteristics of GaN-on-Si green micro-LED for wide color gamut display and high-speed visible light communication. *ACS Photonics*; 2022, 10(1): 92 – 100.
7. Ray-Hua R, et al. Study on the effect of size on InGaN red micro-LEDs. *Scientific reports*; 2022, 12(1): 1324.
8. Shin-Song C, Paul C.-P. C. A high 5292-PPI pixel circuit for micro displays with 10-bit gray levels realized via the technique of analog sub-frame integral. *IEEE Journal of the Electron Devices Society;* 2023, 11: 456 – 466.
9. Hyeon-Jun S, Yong-Duck K, Byeong-Deok C. 4670-PPI OLEDoS pixel circuit design for wide data voltage range in a 5 V 0.13 μm CMOS process, *Journal of the Society for Information Display*; 2024, 32(5): 165 – 173.
10. Xinxin H, Congwei L, Min Z, Hailong J, Shengdong Z. A pixel circuit with wide data voltage range for OLEDos microdisplays with high uniformity. *IEEE Transactions on Electron Devices*; 2019, *66*(11): 4798 – 4804.
11. Bong-Choon K, Han-Sin L, Oh-Kyong K. Organic light-emitting diode-on-silicon pixel circuit using the source follower structure with active load for microdisplays. *Japanese Journal of Applied Physics*; 2011, 50(3S): 03CC05.
12. Kyeong-Soo K, Ji-Hwan P, Jimin K, Chanjin P, Changwon J, Soo-Yeon L. A compact amorphous In-Ga-Zn-oxide thin film transistor pixel circuit with two capacitors for active matrix micro light-emitting diode displays. *IEEE Journal of the Electron Devices Society*; 2023, 11*:* 204 – 209.